Analysis of Sea Spikes in NetRad Clutter

Riccardo Palamà, Maria Greco, Pietro Stinco, Fulvio Gini
Dipartimento di Ingegneria dell'Informazione
University of Pisa
Via G.Caruso16, 56122, Pisa, Italy
e-mail: riccardo.palama@for.unipi.it; {m.greco, pietro.stinco, f.gini}@iet.unipi.it

***Abstract* — In this work our attention is focused on the statistical and spectral analysis of sea clutter spikes recorded by the netted radar system, NetRad, which works in both monostatic and bistatic configurations. Once separated the spikes from the background, we examine their properties, focusing on the spike width and on the interval which separates two consecutive spikes. The spectral properties of the sea spikes are also examined and compared with the background.**

Keywords—sea spikes; sea clutter; bistatic radar; NetRad

I. INTRODUCTION

In recent years growing attention has been devoted to the characterization of sea clutter received by a bistatic radar system. Some recent works have analyzed the bistatic clutter both statistically and spectrally [1][2], but the presence of spikes, which are powerful bursts of clutter samples, has not been thoroughly examined. It has been demonstrated that sea spikes are strongly related to breaking waves [3] and can be separated from the Bragg scattering, which is a "background" component, modulated by the sea swell. The main features that distinguish sea spikes from the Bragg background are their high power, large Doppler velocity and high polarization ratio[4][5].

The analyzed datasets were collected with the NetRad - an abbreviation of Netted Radar - which is a system developed and owned by the University College London [1][7]. The NetRad is a coherent radar, composed by a monostatic and a bistatic node, working at a carrier frequency of 2.4 GHz, a pulse repetition frequency (PRF) of 1 KHz and a range resolution of about 3 m. The radar works at horizontal (HH) or vertical (VV) polarization. The antennas have a beamwidth of 9° (elevation) x 11° (azimuth) and are pointed with different azimuth angles and grazing angle of 1°. The geometry consists in an isosceles triangle, created by the monostatic node, the bistatic node and the intersection point between their antenna patterns[2][7]. For the analyzed dataset the baseline is 728 m and the azimuth angle is 75°, then the range interval of high bistatic clutter goes approximately from 1000 m to 1400 m. The measurements were made at Scarborough, Cape Town, in South Africa on October 21, 2010. The radar was facing the Atlantic Ocean and was located on a bay, the wind and wave direction was approximately from the North-West and the sea state was 4-5 [8]. We analyzed four datasets: bistatic HH, monostatic HH, bistatic VV and monostatic VV data. Each file dimension is $N_p \times N_s$, where N_p=130000 is the number of pulse repetition intervals, and N_s=1024 is the number of samples per sweep (range cells).

The paper is organized as follows. In Section II we illustrate the Power-Range-Time diagrams of the analyzed data and the method used to select the sea spikes from the background component. In Section III we present the results of the statistical analysis of sea spikes, focusing on the properties of the sea spikes duration and the time interval between two subsequent spikes. In Section IV some spectral properties of the sea spikes are examined. Conclusions and final remarks are reported in Section V.

II. SEA SPIKES CLASSIFICATION

In this section a preliminary analysis is provided, in order to have a general view of the sea clutter data, then the sea spikes classification method is described and its results are showed.

Fig.1 shows the Power-Range-Time diagrams of the received data. The analyzed range interval is along the vertical axis, and was set corresponding to the range interval where bistatic clutter-to-noise ratio (CNR) is higher. The horizontal axis corresponds to the time in seconds (data were considered for their entire duration) and the color scale gives the power in dBm. The power maps of bistatic data are characterized by bands of high and low power, which may be noted also in monostatic maps, but more smoothed than the bistatic ones. The bands represent the sea swell. In addition, the presence of peaks with high power, i.e. sea spikes, may be noted mostly in the HH polarized data, whereas the banded pattern shows a more uniform power level in the VV polarized data. Spikes are contained within the high-power bands, meaning that they mainly occur on the crests of the sea waves. The behavior of the monostatic and bistatic data depending on the polarization is similar to that showed by authors in [3] for monostatic clutter, since in general spikes occur mainly in horizontally polarized data.

The classification of spikes was realized by using the algorithm illustrated in [6]. Spikes are short bursts of echoes with an amplitude much higher than the background. Due to this observation, three parameters have been used to define a spike.

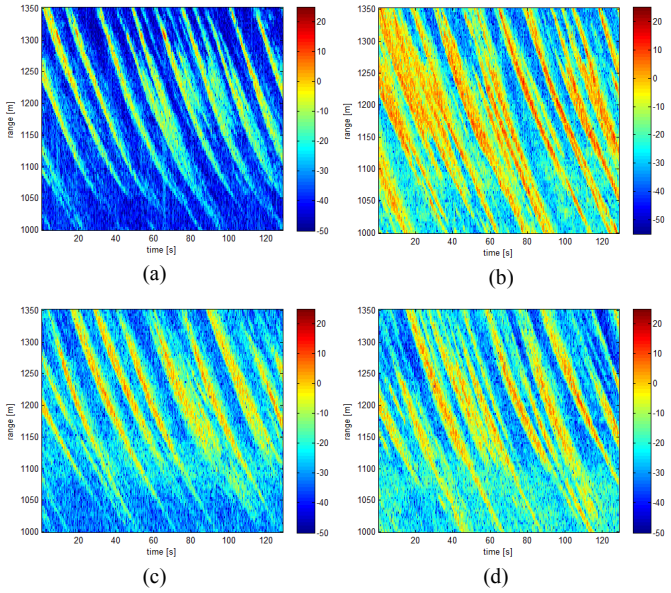

Fig. 1. Power-Range-Time maps: Bistatic HH (a), Monostatic HH (b), Bistatic VV (c), Monostatic VV (d)

The first parameter is the spike amplitude, defined so that the amplitudes of the returns must exceed a power threshold. The parameters used in the following classification step are the minimum spike width (d_{min}) and the minimum interval between spikes (i_{min}). Those sets of samples which last longer than d_{min} are classified as spikes, and those spikes which are separated by an interval smaller than i_{min} are joined together to form one spike. The power threshold was set as 6 times the mean power of the received returns, the minimum spike width was 80 ms and the minimum interval between spikes was 150 ms. These values were chosen empirically. The result of the classification of sea-spikes received by the bistatic node in vertical polarization is shown in the mask in Fig.2, where a value of 1 (white) is associated to a spike and 0 (black) to a pixel belonging to the background. It can be noted that there is a good match between the white areas in Fig.2 and the high-power areas in Fig. 1a, confirming that spikes are mainly concentrated on the crests of the sea waves.

III. Statistical Analysis

Once the sea spikes are separated from the background, it is possible to analyze their statistical properties. First, we analyze the statistical distribution of the spike width and of the time interval between spikes, by evaluating the histograms of the datasets and comparing them with the exponential probability density function (pdf). In detail, the theoretical pdf of the spike width, denoted as $p_D(d)$ in (1), is a one-sided exponential, shifted by d_{min}, with the same mean value of its empirical pdf, denoted as $\bar{d}$.

$$p_D(d) = \frac{1}{\bar{d}} exp\left(-\frac{d-d_{min}}{\bar{d}}\right) u(d-d_{min}) \qquad (1)$$

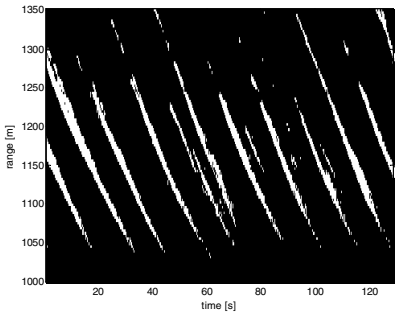

Fig. 2. Mask of selected sea spikes for the bistatic HH clutter data

Similarly, the theoretical pdf of the interval between spikes, $p_I(i)$ in (2), has the same mean value of the data, $\bar{i}$, and is shifted by i_{min}.

$$p_I(i) = \frac{1}{\bar{i}} exp\left(-\frac{i-i_{min}}{\bar{i}}\right) u(i-i_{min}) \qquad (2)$$

Fig.3a and Fig.3b show a good fitting between the empirical pdf of the spike width and the exponential pdf for the HH polarized data. For VV data some deviations can be noted only for small values of the spike width. The results concerning the monostatic data are not plotted since they are similar to those obtained with bistatic data (at least in the shape). In addition, Fig.3c and Fig.3d show that the exponential distribution can model the distribution of the interval between spikes for monostatic data, but in case of bistatic data there are some deviations for values of i included between 10 and 15 seconds.

Some important information about the spikiness of each data can be extracted from Table I, which contains the values of the mean spike width, the mean interval between spikes and the ratio between the number of samples belonging to a spike (N_{sp}) and the number of received samples (N_s). The number of spikes is lower in bistatic data than in monostatic ones, but the difference is very small in case of vertical polarization. For the bistatic data it can be noted that spikes are separated by larger intervals for VV polarization than for HH polarization, even though the width and the number of spikes are smaller for HH data. In other word, the analysis reveals that spikes last longer and are less frequent in the bistatic configuration. A comparison between the two polarizations reveals that the HH polarized data have shorter and more separated spikes than VV data, both for bistatic and monostatic node.

TABLE I. Sea Spikes Statistics

	Bi HH	**Mono HH**	**Bi VV**	**Mono VV**
N_{sp}/N_s	0.0841	0.1325	0.1187	0.1217
$\bar{d}$ [s]	0.9345	0.7503	1.2151	1.0007
$\bar{i}$ [s]	12.2223	6.5142	14.1277	8.5606

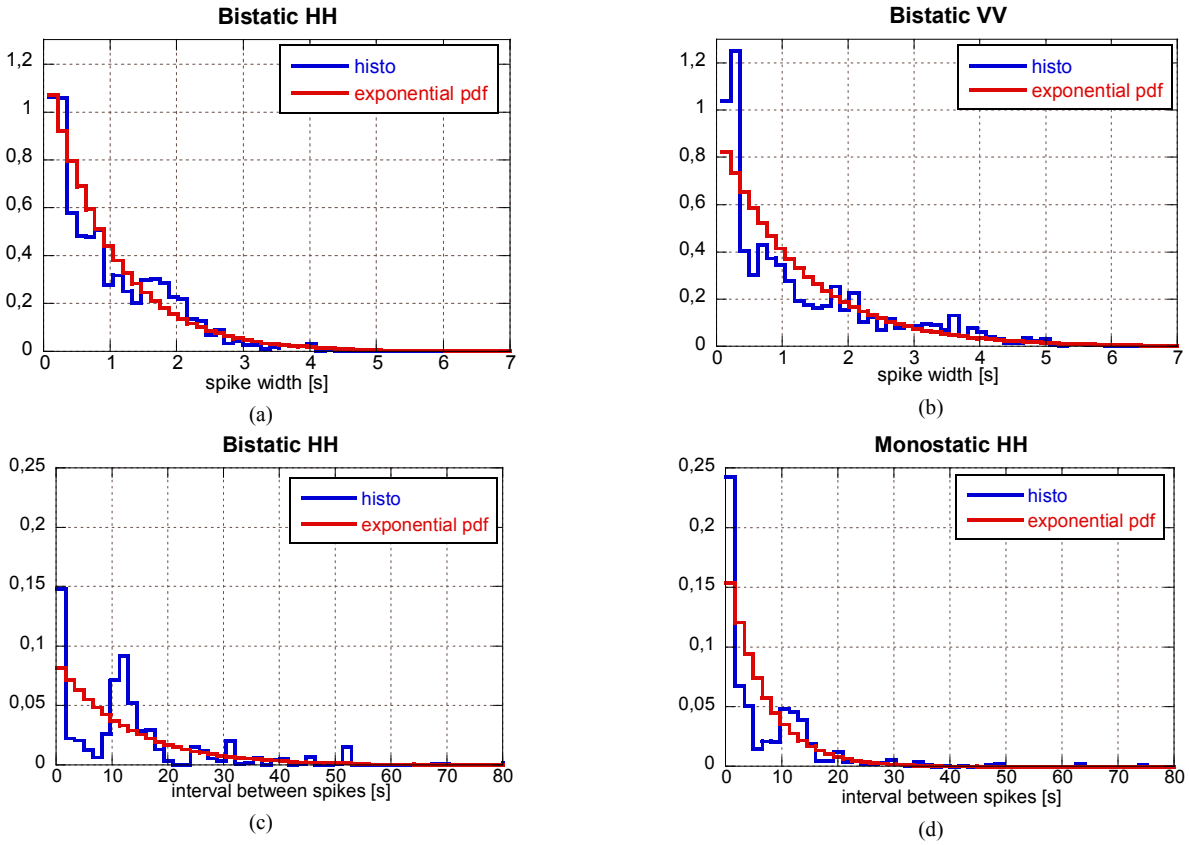

Fig. 3. Histograms of the spike width, Bistatic HH data (a) , Bistatic VV data (b). Histograms of the time interval between spikes, Bistatic HH data (c), Monostatic HH data (d).

IV. Spectral Analysis

In this Section we analyze the spectral properties of the sea spikes: their estimated Power Spectral Density (PSD) was compared with the PSD of the whole data and with the PSD of the background. The considered range interval goes from 1000 m to 1350 m, corresponding to the area of high bistatic CNR, and gives a number of range cells N_c equal to 105. For each range cell, the sequences of samples to analyze were first divided into bursts, with an overlap of 50%, then the periodogram of each burst was computed. The length of a time burst N was set as 1024, since the mean spike width of all the data is close to 1 second, then 1000 temporal samples. In other words, the N_p samples received in each range cell were divided into $2N_p/N$ bursts of length N, for a total of $N_c(2N_p/N)$ segments. For each of these segments the PSD was estimated using the periodogram method, that is, by calculating

$$\hat{S}_{k,m}(f) = \frac{1}{N}\left|\sum_{l=m}^{m+N-1} z_k(l) e^{-j2\pi fl}\right|^2 \qquad (3)$$

where $\hat{S}_{k,m}(f)$ is the PSD estimate of the m^{th} burst of the k^{th} range cell, $m=1,2,...,2N_p/N$ and $k=1,2,...,N_c$.

For a fixed Doppler frequency, the frequency of occurrence of the values of the spectrum was measured, in order to build a map of histograms of the estimated PSD. The spectral analysis was completed by averaging the spectra for each Doppler frequency. In Fig.4 the mean spectra are superimposed on the map of the histograms of the total spectrum, where the average PSD of the background is plotted in white, the one of the spikes in magenta and the one of all the received samples in black. All the spectra are centered on a positive value of normalized Doppler frequency, close to 0.1 Hz, and have a bandwidth of about 0.2 Hz. The value of the center frequency is justified by the fact that the direction of the sea waves is almost parallel to the baseline and directed towards the radar, then both the bistatic and monostatic Doppler frequencies are expected to be slightly higher than zero. In general the spectra of the bistatic sea spikes have one peak at positive Doppler, whereas the monostatic spikes have also a small peak at negative Doppler. The spectra of all the received samples and of the background show a peak at zero Doppler, which is not present in the spectra of sea spikes. This is probably ground clutter, coming from a cliff located behind the two radar receivers. In addition, the Doppler spectra of the sea spikes are always wider than the others. This result confirms a quite good classification of the sea spikes, since they are a fast-moving component, then expected to have a wide Doppler spectrum centered on a frequency larger than the background. The samples of the spectrum of the bistatic HH data are more distributed in the vertical axis (power) than the monostatic HH, which are more concentrated. Furthermore, in HH data most spectrum samples are concentrated within the peak of the spectrum, whereas for the VV data, there is a bigger number of samples on the sides of the spectrum.

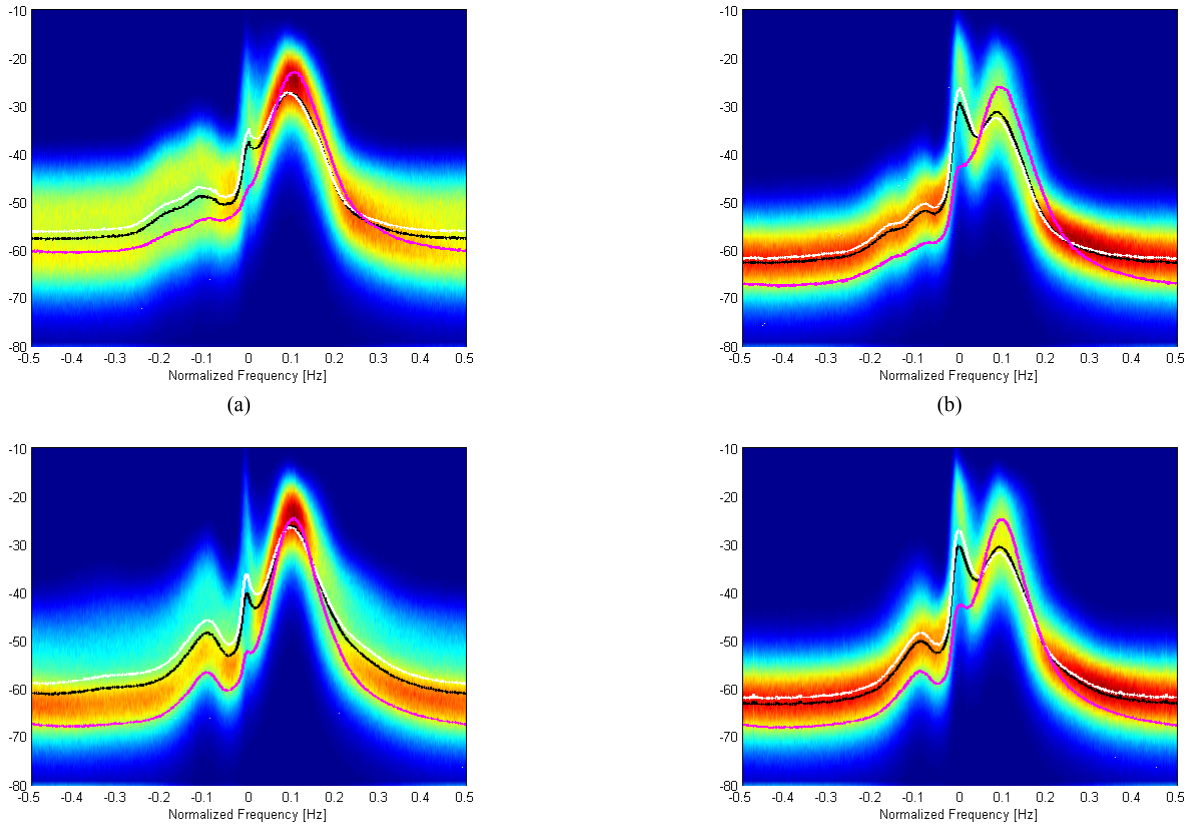

Fig. 4. Frequency of occurrence of the PSD of radar returns and average PSD of the background (white), of the spikes (magenta) and of all the radar returns (black): Bistatic HH data (a), Bistatic VV data (b), Monostatic HH data (c) and Monostatic VV data (d).

This behavior is justified by the fact that VV data are more influenced by the background component. Nevertheless, the average PSD of sea spikes is wider for bistatic data than for monostatic one, and this behavior is evident mostly in VV polarized data.

V. Conclusion

The analysis of sea spikes illustrated in this work has been realized on sea clutter data recorded by a netted monostatic-bistatic radar system. In first analysis, the Power-Range-Time maps have showed that the bands of high and low power, which can be associated to the sea swell, are mostly evident in bistatic data. The statistical properties of the spike width and of the interval between spikes have been examined, and it has been noted that spikes last longer and are less frequent in bistatic data, compared with monostatic. Finally, the frequencies of occurrence of the PSD values of radar returns and the average spectra of the background, of the spikes and of all the radar returns have showed that sea spikes in bistatic VV have a wider spectrum than monostatic VV. The future research activity will deal with the analysis of the properties of bistatic sea spikes depending on the azimuth pointing angle.

Acknowledgments

The authors would thank the University College London and the University of Cape Town, that provided the analyzed data.

References

[1] M.A. Ritchie; W.A.Al-Ashwal.; A.G. Stove; K. Woodbridge; H.D. Griffiths, "Coherent analysis of horizontally-polarized monostatic and bistatic sea clutter", *Proceedings of the IET International Conference on Radar Systems (Radar 2012),* 1-5, Glasgow, UK, 2012.

[2] R.Palamà, M.Greco, P.Stinco, F.Gini; "Statistical analysis of NetRad high resolution sea clutter", *Proceedings of the 21st European Signal Processing Conference (EUSIPCO 2013),* Marrakech, Morocco, 2013.

[3] H.W Melief; H.Greidanus; P.Van Genderen; P. Hoogeboom; "Analysis of sea spikes in radar sea clutter data", *IEEE Transactions on Geoscience and Remote Sensing*, 44, 4 (2006), 985-993.

[4] F.Posner; K.Gerlach; "Sea spike demographics at high range resolutions and very low grazing angles", *Proceedings of the 2003 IEEE Radar Conference*, 38-45, Huntsville,USA, 2003.

[5] M.Greco; P.Stinco; F.Gini; "Statistical analysis of sea clutter spikes", *Proceedings of the European Radar Conference (EuRAD 2009),*192-195, Rome, Italy, 2009.

[6] M.Greco; P.Stinco; F.Gini; "Identification and analysis of sea radar clutter spikes", *IET Radar, Sonar & Navigation* , 4,2 (2010), 239-250.

[7] M. Inggs, Balleri, A., Al-Ashwal, W. A., Ward, K. D., Woodbridge, K., Ritchie, M., Miceli, W., Tough, R. J A, Baker, C. J., Watts, S., Harmanny, R., Stove, A., Sandenbergh, J. S., Griffiths, H.D., "NetRAD multistatic sea clutter database", *Proceedings of the IEEE International Geoscience and Remote Sensing Symposium (IGARSS 2012)*, 2937-2940, Munich,Germany, 2012.

[8] Weather Forecast and Reports, www.wunderground.com .